ELSEVIER

European Journal of Pharmaceutics and Biopharmaceutics 52 (2001) 327–336

European Journal of Pharmaceutics and Biopharmaceutics

www.elsevier.com/locate/ejphabio

Research paper

The effect of powder type, free moisture and deformation behaviour of granules on the kinetics of fluid-bed granulation

Thomas Abberger*

Department of Pharmaceutical Technology, Institute of Pharmacy, University of Innsbruck, Innsbruck, Austria

Received 8 November 2000; accepted in revised form 26 March 2001

Abstract

The effects of two types of powder, lactose and corn starch, and of free moisture on the kinetics of fluid-bed granulation have been investigated using population balance modelling. A coalescence kernel that considered the deformation behaviour of the granules was used. The best fit of the experimental data was obtained for both materials by assuming that the granules underwent plastic deformation. The predicted cumulative number fractions were in very good agreement with the experimental data. The effect of free moisture (in the range of 5–10%) was investigated with lactose. The process was independent of the statistical distribution in free moisture within the approximate range 5–10%. The results suggest a local plasticity in fluid-bed spray granulation caused by the deposition of spray droplets onto the granules, with their subsequent absorption into the voids leading to regions of saturated voids.

Keywords: Deformation behaviour; Fluid-bed granulation; Kinetics; Moisture content; Plasticity; Population balance modelling; Powder type

1. Introduction

Granulation is a key process in the agrochemical, chemical, food, mining and pharmaceutical industries. There is, therefore, a need for the comprehensive modelling of this process from first principles. Modelling is important if one needs to estimate a priori granule characteristics, such as size, shape and density, from a knowledge of the operating conditions and the physical and chemical properties of the powder and binder [1].

There is a clear lack of work dealing with the modelling of granulation in the pharmaceutical literature, despite the large-scale application of this process in the pharmaceutical industry. The work carried out for this paper aimed at investigating the effects of powder type (lactose and corn starch) and the free moisture content of lactose granules on their growth kinetics, with population balance modelling using a kernel which accounted for the deformation behaviour of the granules.

2. Theoretical development

2.1. The population balance equation

The basis for the modelling of granulation is the statistical mechanics equations describing the Markov processes. Examples of linear, irreversible Markovian equations are, for example, the Fokker–Planck, Smoluchowski [2] and master equations. These equations have been quite successful in the codification of large quantities of experimental data on different systems [3]. Müller [4] was probably the first to derive an equation in continuous form describing the coagulation or coalescence of free-in-space systems such as diluted colloidal solutions, given by

$$\frac{\mathrm{d}f(v,t)}{\mathrm{d}t} = -\int_0^\infty \beta(v,u)f(v,t)f(u,t)\mathrm{d}u + \frac{1}{2}\int_0^v \beta(v-u,u)f(v-u,t)f(u,t)\mathrm{d}u \quad (1)$$

where $f(v,t)$ is the number density function, t is time, u and v are the volumes of spherical particles, and $\beta(v,u)$ is the coalescence kernel.

Eq. (1) is a population balance equation (PBE) because it expresses a simple balance: the rate of accumulation of particles of a given size equals their rate of formation minus their rate of disappearance. The left hand side of Eq. (1) represents the time rate of change of the number

* Department of Pharmaceutical Technology, Institute of Pharmacy, University of Innsbruck, Josef-Moeller-Haus, Innrain 52, 6020 Innsbruck, Austria. Tel.: +43-512-507-5373; fax: +43-512-507-2933.

E-mail address: thomas.abberger@uibk.ac.at (T. Abberger).

0939-6411/01/$ - see front matter
PII: S0939-6411(01)00185-0

of particles with volume v. The first term on the right hand side of Eq. (1) describes the rate of disappearance of particles with volume v by their collision and binding with another particle of any diameter. The second term represents the rate of formation of particles with volume v by the collision and binding together of two particles whose two volumes total v. The leading factor of 1/2 is added to avoid any double counting.

A PBE relates to the particle size distribution, the system kinetics, the device, the operating conditions and the material flows [5]. PBEs allow an analysis of how particle size distributions are related to the underlying microscopic kinetics.

For a restricted-in-space system, as in a granulator, the number of random collisions between particles belonging to any two size groups, i and j, under the constraint of perfect mixing is proportional to the product of the number of species of one type with the number fraction of the second type (Eq. (2)) [6].

$$[\text{Collisions}]_{i,j} \propto n_i(t)\frac{n_j(t)}{N(t)} \tag{2}$$

where $N(t)$ is the total number of particles in the system at time t.

Therefore, the right hand side of Eq. (1) has to be divided by the total number of particles, $N(t)$, to describe the population balance in a granulating device (Eq. (3)) [7].

$$\frac{\mathrm{d}f(v,t)}{\mathrm{d}t} = -\frac{1}{N(t)}\int_0^\infty \beta(v,u)f(v,t)f(u,t)\mathrm{d}u$$

$$+\frac{1}{2N(t)}\int_0^v \beta(v-u,u)f(v-u,t)f(u,t)\mathrm{d}u \tag{3}$$

A review of population balance modelling has been carried out by Ramkrishna [8].

2.2. The coalescence kernel

The coalescence kernel is a very important parameter in a PBE, as it gives the functional dependency of the growth rate on the process and the material variables. Owing to the limited knowledge of the forces involved in the granulation process, the kernels available in the literature are only empirical or semi-empirical. A summary of some coalescence kernels has been given by Cryer [9].

Based on a force balance between two colliding granules with diameters D and d, Ouchiyama and Tanaka [10] developed a semi-empirical kernel (Eq. (4)). Successful coalescence occurs if the strength of the formed liquid bridge is greater than the separating forces and is described by a probability, $P(D,d)$, that is a number between 0 and 1.

$$P(D,d) = \lambda^n\left[1-\left\{\frac{(Dd)^{\gamma-3\eta/2}}{\left(\frac{D+d}{2}\right)^{2\gamma-4-3\eta/2}/\delta^{4-3\eta/2}}\right\}^{2/(3\zeta)}\right]^n \tag{4}$$

where δ is a characteristic limiting size, defined as

$$P(D,d) = 0 \text{ for } D \geq \delta;\ d \geq \delta.$$

The kernel requires five semi-empirical constants, namely, γ, η, λ, ζ and n. Two of these constants, η and ζ, are related to the elastic and plastic behaviour of the colliding particles. The surface area of contact, S, between two colliding particles is given by

$$S \propto Q^{\zeta}\left(\frac{Dd}{D+d}\right)^{\eta} \tag{5}$$

where Q is the compressive force between two colliding granules.

According to the theory of Hertz (cf. Refs. [11–13]), values of $\eta = 0$ and $\zeta = 1$ describe plastic behaviour, and values of $\eta = \zeta = 2/3$ describe elastic behaviour [14].

By equating the dissipation of the initial kinetic energy of the colliding granules in a viscous binder layer around the granules, Ennis et al. [15] proposed that coalescence will occur if the initial kinetic energy is dissipated, otherwise the liquid bridge formed from contact of the colliding particles will rupture, and rebound will occur. The critical Stokes number represents the critical energy required for rebound.

Adetayo and Ennis [16] described the limiting size, δ, as a function of the critical Stokes number St* as

$$\delta = \left(\frac{16\mu}{\rho v}\mathrm{St}^*\right) \tag{6}$$

where μ is binder viscosity, ρ is the granule density, v is the initial collision velocity and St* is the critical Stokes number.

Kristensen et al. [17] obtained the following equation for the limiting size, δ:

$$\delta^{2/a} = A\frac{(\Delta l/D)^3}{\sigma_c} \tag{7}$$

where a and A are constants for the given system, D is the diameter of the agglomerate, and $\Delta l/D$ is the normalized strain of the agglomerate caused by a stress corresponding to the compressive strength, σ_c, of the agglomerate.

2.3. Solution of the PBE

Analytical solutions of the PBE are known only for a few, simple kernels [5,18]. For kernels with physical significance, no analytical solutions seem to be possible [19]. In some cases, similarity solutions are possible, which transform the PBE into an ordinary integro-differential equation, thus reducing the number of independent variables from two to one. Such similarity solutions can represent exact solutions over a long time period [19].

Various methods are available to numerically solve a PBE [20]. Their accuracy can be tested with kernels for which the analytical solutions are known.

One PBE, which is formulated in a manner that mass is conserved during the evolution of time, which is not difficult

to program and which is claimed to be relatively accurate, is the discretized population balance of Hounslow et al. [21] (Eq. (8)).

$$\frac{dN_i}{dt} = \frac{1}{N(t)}\left(N_{i-1}\sum_{j=1}^{i-2}2^{j-i+1}\beta_{i-1,j}N_j + \frac{1}{2}\beta_{i-1,i-1}N_{i-1}^2 - N_i\sum_{j=1}^{i-1}2^{j-i}\beta_{i,j}N_j - N_i\sum_{j=i}^{\infty}\beta_{i,j}N_j\right) \quad (8)$$

Here, N_i is the number of particles in the ith interval, $N(t)$ is the total number of particles in the system at time t, and $\beta_{i,j}$ is the coalescence kernel of particles in the ith and jth section.

In the discretized PBE, the partial differentials are replaced with finite differences (except in the time domain), the integrals with sums, and the number density with numbers of particles in defined size ranges [5], which facilitates a solution.

A geometric discretization of the particle size distribution was chosen for formulating Eq. (8) as

$$\frac{v_{i+1}}{v_i} = 2^{1/r} \quad (9)$$

where v_i is the volume of a particle in the ith interval and r is an integer (unity in the case of Eq. (8)).

A geometric discretization requires a fewer number of intervals to describe a particle size distribution than a uniform discretization, where each interval spans the same constant range in particle sizes [5].

To allow a finer discretization than obtainable with the term $v_{i+1}/v_i = 2$, Litster et al. [22] expanded Eq. (8) to include integer numbers greater than unity.

Eq. (8) has to be solved as many times as the number of intervals there are in the division of the particle size distribution. It spans the smallest particle range for the starting powder, up to the largest volume expected for a granule. There should always be an empty interval at the end of the particle size distribution to avoid a finite domain error. A finite domain error can be monitored by checking that $\int_{v_{\min}}^{v_{\max}} vf(v,t)dv$ is conserved during the computations [23].

After numerical calculation of the right hand side of Eq. (8), the integration over dt can be performed using a standard technique.

2.4. Free moisture

According to Abberger and Egermann [24], the amount of free moisture (which can be defined as the ratio of free moisture to the powder mass, in percentage units) is calculated from the difference between the moisture input and the eliminated moisture.

The eliminated moisture is determined both by the humidity in the exhaust air, and by the amount of moisture sorbed by the powder. This latter term may be important with particles that show a swelling characteristic, such as starch powder, where considerable quantities of water are eliminated by absorption. With lactose powder, absorption is not significant. With non-sorbing powders, the free moisture can be calculated from the operating conditions based on a thermodynamic model [25–27].

3. Materials and methods

3.1. Experimental

The experimental details are given in Table 1. Two series of experiments were performed using lactose. The first series was with a target content of 5% free moisture. According to calculations of free moisture from the known operating conditions, 44 ml of the granulating liquid was added at a rate of 30 ml/min to obtain a 5% free moisture level. The spray rate was reduced to the equilibrium value of 11.9 ml/min, and then volumes of 50, 100, 150, 200, 250, 300 or 350 ml were sprayed continuously onto the powder bed.

Table 1
Experimental details

Equipment:	Instrumented [27] fluid-bed granulator, STREA-1 (Aeromatic-Fielder, Bubendorf, Switzerland) for batchwise operation
Feed material:	Lactose Ph. Eur. grade, GranuLac 200 (Meggle, Wasserburg, Germany); corn starch, Maisita 21005 (Agena, Wien, Austria)
Batch size:	400 g
Granulating fluid:	Aqueous solution of 4% polyvinylpyrrolidone Ph. Eur. grade, Kollidon® 90 F (BASF, Ludwigshafen, Germany)
Laboratory air conditions:	Temperature, 20 ± 1°C; relative humidity, 45 ± 10%
Inlet air flow rate:	40 m^3/h
Inlet air temperature:	70°C
Atomizing air pressure:	0.8 bar
Nozzle diameter:	0.8 mm
Calculated equilibrium spray rate [26]:	11.9 ml/min

The second series was with a target content of 10% free moisture. In this case, 78 ml of liquid was added at a rate of 30 ml/min. Then, volumes of 50, 100, 150, 200 or 250 ml were sprayed onto the powder bed at a rate of 11.9 ml/min.

For each granulation, samples weighing about 5 g were taken after the addition of the first 44 or 78 ml, respectively, and after the addition of the total volume of granulating liquid. These samples were dried using a moisture analyzer LP 16 (Mettler, Greifensee, Switzerland) [27], and the free moisture was calculated from the loss on drying.

With the corn starch, two experimental series were also performed [28]. With the first series, 150, 200, 250, 300 or 375 ml of granulating liquid was sprayed onto the powder bed at a rate of 20 ml/min.

With the second series, 200 ml of pure water was sprayed at a rate of 20 ml/min on each batch. Subsequently, 250, 300 or 350 ml of 4% polyvinylpyrrolidone solution was sprayed at a rate of 20 ml/min onto the batch.

Owing to the difficulties in being able to tell the free moisture from sorbed moisture when determining the loss on drying, no experimental data on the free moisture can be given for the starch granulations. Starch was chosen because it is practically insoluble in cold water [29].

The size distributions of 100 g for the dried starch granules and 250 g for the dried lactose granules were determined by sieve analysis [25]. The sieve analysis data were fitted to a log-normal distribution function using a program developed by Spencer and Lewis [30]. This determined the median diameter, $d_{50,3}$, the geometric standard deviation, s_g, and the coefficient of correlation, R^2, of the data from the log-normal distribution function. The standard deviation, s, defined as $s = \ln(d_{84}/d_{50})$, was calculated according to the

Table 2
Number of particles in each class at selected values of τ for a lactose series (target content of 5% free moisture)

Class	Ub[a]	τ						
		0 (start)	0.1	0.5	1.0	1.5	2.1	3.0
1	1.6	0.00E + 00	0.00E + 00	0.00E + 00	0.00E + 00	0.00E + 00	0.00E + 00	0.00E + 00
2	2.0	0.00E + 00	0.00E + 00	0.00E + 00	0.00E + 00	0.00E + 00	0.00E + 00	0.00E + 00
3	2.5	0.00E + 00	0.00E + 00	0.00E + 00	0.00E + 00	0.00E + 00	0.00E + 00	0.00E + 00
4	3.2	0.00E + 00	0.00E + 00	0.00E + 00	0.00E + 00	0.00E + 00	0.00E + 00	0.00E + 00
5	4.0	0.00E + 00	0.00E + 00	0.00E + 00	0.00E + 00	0.00E + 00	0.00E + 00	0.00E + 00
6	5.0	0.00E + 00	0.00E + 00	0.00E + 00	0.00E + 00	0.00E + 00	0.00E + 00	0.00E + 00
7	6.3	0.00E + 00	0.00E + 00	0.00E + 00	0.00E + 00	0.00E + 00	0.00E + 00	0.00E + 00
8	8.0	0.00E + 00	0.00E + 00	0.00E + 00	0.00E + 00	0.00E + 00	0.00E + 00	0.00E + 00
9	10.1	0.00E + 00	0.00E + 00	0.00E + 00	0.00E + 00	0.00E + 00	0.00E + 00	0.00E + 00
10	12.7	0.00E + 00	0.00E + 00	0.00E + 00	0.00E + 00	0.00E + 00	0.00E + 00	0.00E + 00
11	16.0	0.00E + 00	0.00E + 00	0.00E + 00	0.00E + 00	0.00E + 00	0.00E + 00	0.00E + 00
12	20.2	0.00E + 00	0.00E + 00	0.00E + 00	0.00E + 00	0.00E + 00	0.00E + 00	0.00E + 00
13	25.4	0.00E + 00	0.00E + 00	0.00E + 00	0.00E + 00	0.00E + 00	0.00E + 00	0.00E + 00
14	32.0	5.71E + 04	5.21E + 04	3.59E + 04	2.25E + 04	1.41E + 04	7.98E + 03	3.40E + 03
15	40.3	9.92E + 04	9.06E + 04	6.31E + 04	3.99E + 04	2.52E + 04	1.45E + 04	6.25E + 03
16	50.8	2.34E + 05	2.15E + 05	1.52E + 05	9.77E + 04	6.26E + 04	3.65E + 04	1.61E + 04
17	64.0	5.11E + 05	4.71E + 05	3.39E + 05	2.24E + 05	1.46E + 05	8.75E + 04	3.99E + 04
18	80.6	1.23E + 06	1.14E + 06	8.46E + 05	5.76E + 05	3.89E + 05	2.41E + 05	1.15E + 05
19	101.5	1.62E + 06	1.52E + 06	1.17E + 06	8.31E + 05	5.85E + 05	3.80E + 05	1.94E + 05
20	127.9	2.86E + 06	2.70E + 06	2.16E + 06	1.61E + 06	1.19E + 06	8.19E + 05	4.55E + 05
21	161.2	4.21E + 06	4.03E + 06	3.38E + 06	2.68E + 06	2.10E + 06	1.54E + 06	9.44E + 05
22	203.1	4.21E + 06	4.09E + 06	3.63E + 06	3.09E + 06	2.59E + 06	2.06E + 06	1.41E + 06
23	255.9	3.76E + 06	3.70E + 06	3.45E + 06	3.12E + 06	2.79E + 06	2.39E + 06	1.84E + 06
24	322.4	4.51E + 06	4.46E + 06	4.27E + 06	4.01E + 06	3.73E + 06	3.38E + 06	2.85E + 06
25	406.1	2.71E + 06	2.71E + 06	2.72E + 06	2.71E + 06	2.68E + 06	2.62E + 06	2.47E + 06
26	511.7	1.92E + 06	1.93E + 06	1.94E + 06	1.96E + 06	1.97E + 06	1.98E + 06	1.97E + 06
27	644.7	1.23E + 06	1.24E + 06	1.25E + 06	1.27E + 06	1.29E + 06	1.31E + 06	1.35E + 06
28	812.2	5.20E + 05	5.23E + 05	5.33E + 05	5.46E + 05	5.61E + 05	5.80E + 05	6.10E + 05
29	1023	2.28E + 05	2.29E + 05	2.32E + 05	2.36E + 05	2.40E + 05	2.46E + 05	2.56E + 05
30	1289	9.92E + 04	0.00E + 00	1.00E + 05	1.01E + 05	1.03E + 05	1.04E + 05	1.07E + 05
31	1624	5.41E + 04	0.00E + 00	5.44E + 04	5.46E + 04	5.50E + 04	5.54E + 04	5.61E + 04
32	2046	0.00E + 00	0.00E + 00	1.34E + 02	2.83E + 02	4.47E + 02	6.64E + 02	1.03E + 03
33	2578	0.00E + 00	0.00E + 00	1.19E-01	4.97E-01	1.22E + 00	2.66E + 00	6.38E + 00
34	3248	0.00E + 00	0.00E + 00	4.52E-05	3.76E-04	1.42E-03	4.56E-03	1.70E-02
35	4093	0.00E + 00	0.00E + 00	0.00E + 00	0.00E + 00	0.00E + 00	0.00E + 00	0.00E + 00
Sum		3.01E + 07	2.91E + 07	2.63E + 07	2.32E + 07	2.05E + 07	1.79E + 07	1.47E + 07

[a] Ub, upper bound of class (μm).

Table 3
Properties of the lactose granulations

Volume of granulating liquid (ml)	Free moisture content (%)			Granule size	
	Target	Start	End	$d_{50,0}$ (μm)	s
44 + 100	5	6.4	6.0	202	0.63
44 + 150	5	5.1	3.9	279	0.56
44 + 350	5	ND[a]	5.5	323	0.64
78 + 50	10	10.2	9.2	138	0.77
78 + 100	10	5.6	6.0	288	0.57
78 + 150	10	9.7	7.5	410	0.48
78 + 200	10	11.4	7.8	469	0.47
78 + 250	10	8.0	8.5	465	0.47

[a] ND, not determined.

relation, $s = \ln s_g$. The median diameter of the number distribution, $d_{50,0}$, was calculated using a Hatch–Choate Equation [31].

3.2. Modelling

To model granule growth with the population balance approach, the following assumptions were used (assumptions (i)–(iii) cf. Ref. [12]):

(i) that the particles in the granulator are completely mixed, and coalescence occurs by the combination of two particles;

(ii) that coalescence occurs whenever an adhesive force is experienced by a pair of particles;

(iii) that attrition or crushing of the granules can be disregarded; and

(iv) that the evolution of porosity can be disregarded.

In each of the lactose series, the first granulation with an R^2 value of at least 0.99 was used as the starting distribution for the simulation. These were the 44 + 100 ml for the 5% series, and the 78 + 50 ml for the 10% series. The starting distribution for the starch series in Fig. 3 was the granulation with 150 ml of added granulating liquid, and this with 250 ml for the series in Fig. 4.

The total number of particles of the starting distribution, $N(t_0)$, was calculated according to the equation

$$N(t_0) = m_b \frac{6}{\pi d_{vn}^3 \rho_a} \tag{10}$$

where m_b is the mass of the batch in grams, d_{vn} is the diameter, from the arithmetic mean of volume distribution in centimetres, and ρ_a is the apparent density in grams per cubic centimetre.

The value of d_{vn} was calculated from sieve analysis data using a Hatch–Choate Equation.

The apparent densities from measurements by Nimylowytsch [32] were used for the computation of $N(t_0)$, which was 1.00 g/cm^3 in the case of the example shown in Table 2.

A dimensionless time, τ, was introduced according to

$$\tau = qt \tag{11}$$

where q is the frequency of the adhesion force experienced by a pair in reciprocal seconds, and t is real time in seconds.

To resolve the particle size distribution determined by the sieve analysis, taking a value for $r = 1$ was sufficient, and therefore Eq. (8) was used in its original form in this work.

Eq. (8) was integrated using the Runge–Kutta 4th Order technique with $d\tau = 0.1$, and the coalescence kernel of Ouchiyama and Tanaka [10] (Eq. (4)) was also applied. All the calculations were performed using a Microsoft Excel spreadsheet.

Table 2 shows an example of a run (the lactose series with a target content of 5% free moisture). It shows the number of particles in each class at selected values of dimensionless time, τ. The best fit between the model and the experimental data was obtained for values of τ of 2.1 and 3.0, where $\tau = 2.1$ corresponds to 4 min 12 s, and $\tau = 3.0$ corresponds to 21 min in real time.

A monotonic function with a decreasing gradient described the relationship between τ and t very well when τ and t were fitted using the TableCurve 2D software package (SPSS, Chicago, IL), as was found empirically for each of the four series.

Table 4
Properties of the starch granulations

Volume of granulating liquid (ml)	Granule size	
	$d_{50,0}$ (μm)	s
150	32	0.72
200	51	0.71
250	67	0.70
300	124	0.56
375	163	0.67
After addition of 200 ml pure water		
250	38	0.99
300	87	0.82
350	94	0.79

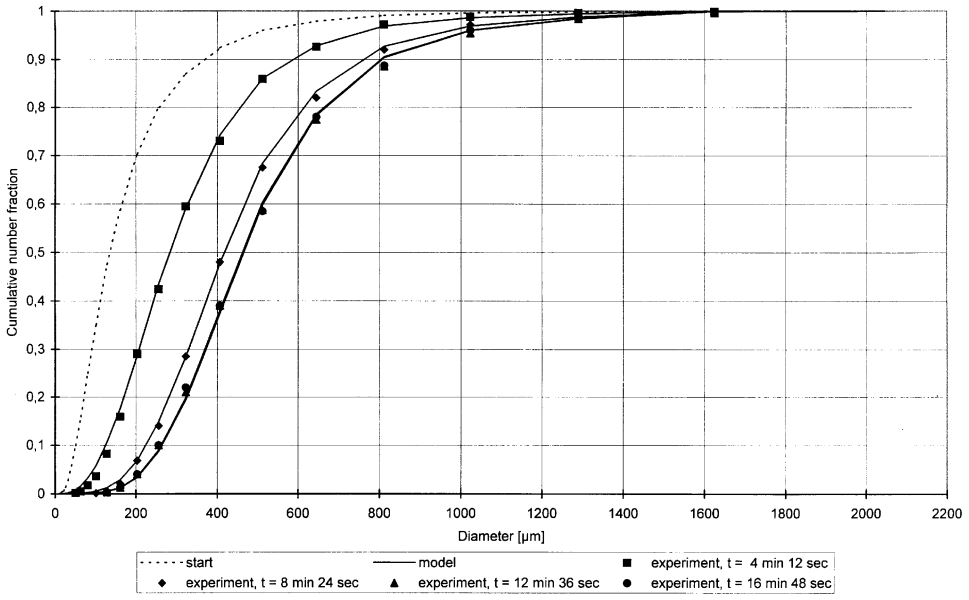

Fig. 1. Predicted and experimental cumulative number distribution of the lactose 10% series.

4. Results

Table 3 shows the properties of the lactose granulations used in the fitting experiments the $d_{50,0}$ and s values and the target and measured free moisture contents after 44 or 78 ml, respectively, of added granulating liquid (start) and at the end of the process of adding the granulating liquid. The deviations from the target contents reflect the experimental difficulties in obtaining the desired moisture content. Table 4 shows the $d_{50,0}$ and s values for the starch granulations.

Fig. 1 shows the evolution of the cumulative number distribution with time for the 10% series and Fig. 2 shows the evolution for the 5% series. Fig. 3 shows the evolution of the cumulative number distribution for the starch granulations without any previously added water and Fig. 4 shows the evolution of the cumulative number distribution for the starch granulations with a previous addition of 200 ml of pure water. Only these granulations were considered for comparison with the model, as R^2 from the log-normal distribution had a value of at least 0.99. This was true for the lactose granulations in Table 3, and for all of the starch granulations. This limitation was necessary, because a number distribution had to be obtained from the sieve analysis data.

The fit between the model and the data is very good (see Tables 5 and 6), except for one curve shown in Fig. 3. Here,

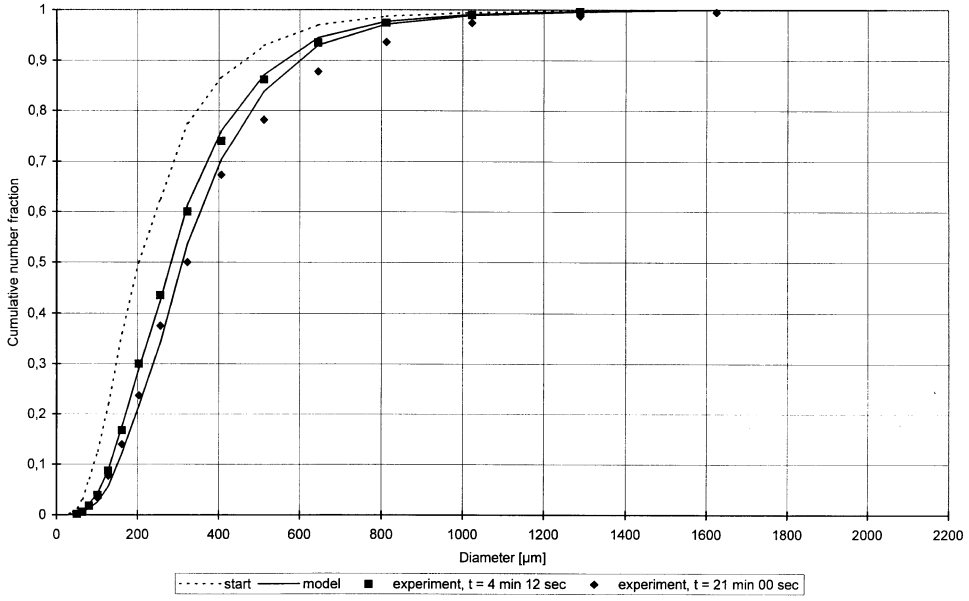

Fig. 2. Predicted and experimental cumulative number distribution of the lactose 5% series.

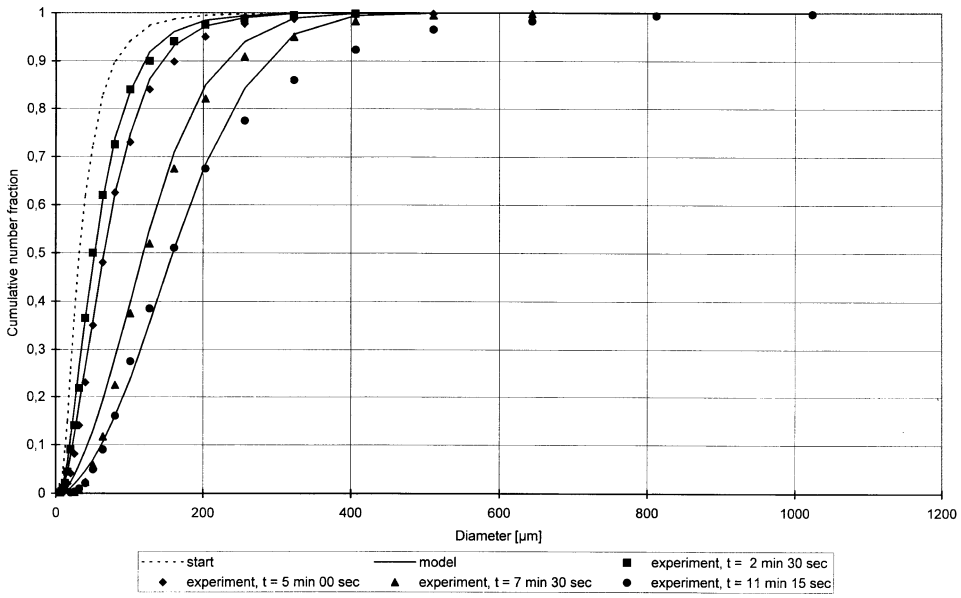

Fig. 3. Predicted and experimental cumulative number distribution of the starch series.

the model underestimated the coarsest fractions for the process after 11 min 15 s; however, the 375 ml granulating liquid additive was near to the limit that could be added under the applied experimental conditions before overwetting and defluidization occurred.

With the assumption that the granules underwent plastic deformation, the evolution of the size distribution could be modelled well for both materials. With lactose, the evolution could be modelled well independent of the statistical distribution that existed between 5 and 10% of the free moisture content within each series (see Table 3). The best fit of the model to the data was obtained using values of $\zeta = 1$, $\lambda = 1$, $\gamma = 9$ and $n = 5$ as the model parameters for all the granulations. These four values are within the limits of the coalescence probability model [33].

When using a value of $\eta = 2$, the best fit was obtained for the lactose series and the starch series with previously added water. For the starch series without added water, the best fit was obtained using $\eta = 0$ (see Tables 5 and 6).

In the best fit, δ was constantly equivalent to 2900 μm for both lactose series, and constantly equivalent to 1100 μm for both starch series. Cryer [9] related the value of δ to the fluidization conditions, as they affect the relative collisional velocity of the particles and, therefore, the Stokes number.

For each of the four series, the dimensionless time, τ, was a monotonic function of the real time, t, with decreasing

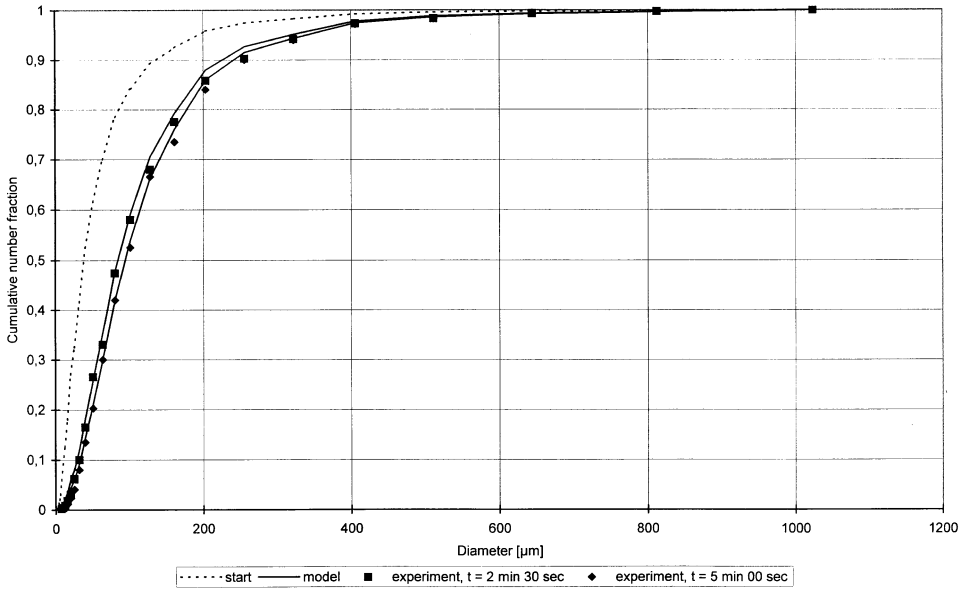

Fig. 4. Predicted and experimental cumulative number distribution of the starch series with previous addition of 200 ml pure water.

Table 5
Values used in the simulation of the lactose series, and the coefficient of correlation between the predicted and the experimental size distribution

Free moisture	5%		10%			
Time, t	4 min 12 s	21 min 00 s	4 min 12 s	8 min 24 s	12 min 36 s	16 min 48 s
ζ	1	1	1	1	1	1
η	2	2	2	2	2	2
λ	1	1	1	1	1	1
γ	9	9	9	9	9	9
n	5	5	5	5	5	5
δ (μm)	2900	2900	2900	2900	2900	2900
R^2	0.9997	0.9976	0.9998	0.9998	0.9996	0.9994

gradient. This indicates that, at least under the applied fluidization conditions, q is not constant during the course of a fluid-bed granulation. For further elucidation additional work will need to be carried out.

5. Discussion

Liu et al. [34] stressed that neither the approach of Ouchiyama and Tanaka [10], nor that of Ennis et al. [15] is completely satisfactory. Ennis et al. [15] neglected the role of plastic deformation at the contact point, and did not consider non-surface wet granules. Liu et al. [34] extended the model of Ennis et al. [15] by additionally accounting for plastic deformation in the granule matrix. The Ouchiyama and Tanaka [10] coalescence kernel is applicable in simulations of the data of this work; however, the general applicability of this type of modelling has not yet been documented.

The starch series without the previous addition of water could be simulated best when using values of $\zeta = 1$ and $\eta = 0$. According to the literature [11,12,33], these values stand for plastic deformation of the granules. The other three series gave the best fit when using values of $\zeta = 1$ and $\eta = 2$.

Values higher than 2/3 for η may result from a probable positive size dependence on the compressive force, which was discarded in formulating the coalescence probability [33]. However, this work shows experimental evidence that this should be considered. It is not yet clear why this effect is not visible with the starch granulations without any previous addition of pure water.

The best fit was always obtained when $\zeta = 1$, which is indicative of plastic deformation behaviour. Agglomerates have to contain sufficient liquid to render them plastically deformable [35]. In experiments with lactose, the apparent saturation degree required to see significant growth was in the range of about 30–60% [36]. Holm et al. [37] showed that lactose becomes plastically deformable at liquid saturations between 30 and 80%, dependent on the porosity of the sample. From Eq. (7), Kristensen et al. [17] concluded that the rate of growth by coalescence between agglomerates is controlled primarily by the saturation degree of the agglomerate, because it is the liquid saturation which controls the strain behaviour.

In fluid-bed spray granulation, spray droplets that hit the granules spread over their surfaces, and need some time to be absorbed and distributed. The deposition and subsequent absorbance of spray droplets in granules during fluid-bed spray granulation is supposed to dynamically lead to regions of locally high void saturation with increased plastic deformation behaviour, even if the overall saturation of the granulation charge is low, e.g. in the pendular state. If the area where deformation takes place when the granules collide is smaller than or equal to the area of local plasticity, it is likely that one can use a value of $\zeta = 1$, although the overall saturation is low.

Huang and Kono [38] focused on local effects due to the structural heterogeneity of a granule. They stated that the local deformability (defined as the ability for local porosity

Table 6
Values used in the simulation of the starch series, and the coefficient of correlation between the predicted and the experimental size distribution

	Without previous addition of water				With previous addition of water	
Time, t	2 min 30 s	5 min 00 s	7 min 30 s	11 min 15 s	2 min 30 s	5 min 00 s
ζ	1	1	1	1	1	1
η	0	0	0	0	2	2
λ	1	1	1	1	1	1
γ	9	9	9	9	9	9
n	5	5	5	5	5	5
δ (μm)	1100	1100	1100	1100	1100	1100
R^2	0.9985	0.9990	0.9987	0.9948	0.9995	0.9996

reduction) controls granule growth in granules with low moisture contents.

To verify the possible effect of local plasticity, further porosimetry measurements are necessary to estimate the overall saturation. It is unlikely that the local plasticity is completely unaffected by the total moisture content; however, it is likely that it depends on the droplet size, which is another controlling factor in fluid-bed spray granulation [39–42].

Granulation time must always be considered. A corresponding effect in this work is that the binder concentration within the agglomerates is proportional to the operating time. As the water is eliminated from the granulating liquid during the process by evaporation or absorption, the binder concentration, and consequently the viscosity of the liquid bridges within the agglomerates, will increase. Although there may be local variations in binder distribution and thus in viscosity, the viscosity of the surface layer is supposed to increase markedly during the process. According to Ennis et al. [15], the agglomerate growth will be affected by the viscosity. With the lactose powders, a small part will become dissolved in the granulating liquid and act as a second binder.

Acknowledgements

The author acknowledges Mag. Barbara Kraus at the University of Innsbruck for discussions regarding solutions of the PBE, and Dr Ken Morris at the Purdue University, West Lafayette, IN for linguistic advice, and the donations of the lactose from the Meggle company and of the Kollidon 90 F from BASF.

Appendix A. List of symbols

a, A, constants.
d, D, diameter of granule.
d_{vn}, diameter of granule, from the arithmetic mean of volume distribution.
$d_{50,0}$, median diameter of the number distribution.
$f(v,t)$, number density function.
l, strain.
m_b, mass of batch.
n, model parameter in the coalescence probability.
$n_i(t)$, number of particles in size group, i, at time, t.
N_i, number of particles in the ith interval.
$N(t)$, total number of particles in the system at time, t.
P, coalescence probability, defined by Eq. (4).
q, frequency of adhesion force experienced by a pair.
Q, compressive force between two colliding granules.
r, an integer.
s, standard deviation.
s_g, geometric standard deviation.
S, surface area of contact.
St*, critical Stokes number.
t, time.
u, v, volumes of spherical particles.
v, initial collision velocity.
v_i, volume of a particle in the ith interval.
β, coalescence kernel.
δ, characteristic limiting size.
γ, model parameter in coalescence probability.
η, property of a granule.
λ, model parameter in coalescence probability.
μ, binder viscosity.
ρ, granule density.
ρ_a, apparent density of granules.
σ_c, compressive strength.
τ, dimensionless time defined by Eq. (11).
ζ, property of a granule.

References

[1] I. Talu, G.I. Tardos, M.I. Khan, Computer simulation of wet granulation, Powder Technol. 110 (2000) 59–75.
[2] M. von Smoluchowski, Versuch einer mathematischen Theorie der Koagulationskinetik kolloider Lösungen, Z. Phys. Chem. 92 (1918) 129–168.
[3] W.A. Wassam, Statistical mechanics, in: R.A. Meyers (Ed.), 2nd Edition, Encyclopaedia of Physical Science and Technology, 15, Academic Press, San Diego, CA, 1992, pp. 713–765.
[4] H. Müller, Zur allgemeinen Theorie der raschen Koagulation, Kolloidchem. Bech. 27 (1928) 223–250.
[5] M. Hounslow, Masters Course I, University of Sheffield, Sheffield, 2000 http://www.shef.ac.uk/uni/projects/ppg/pbe.htm
[6] P.C. Kapur, D.W. Fuerstenau, A coalescence model for granulation, Ind. Eng. Chem. Process Des. Dev. 8 (1969) 56–62.
[7] P.C. Kapur, K.V.S. Sastry, D.W. Fuerstenau, Mathematical models of open-circuit balling or granulating devices, Ind. Eng. Chem. Process Des. Dev. 20 (1981) 519–524.
[8] D. Ramkrishna, The status of population balances, Rev. Chem. Eng. 3 (1985) 49–95.
[9] S.A. Cryer, Modelling agglomeration processes in fluid-bed granulation, AIChE J. 45 (1999) 2069–2078.
[10] N. Ouchiyama, T. Tanaka, The probability of coalescence in granulation kinetics, Ind. Eng. Chem. Process Des. Dev. 14 (1975) 286–289.
[11] S. Watano, T. Morikawa, K. Miyanami, Kinetics of granule growth in fluidized bed granulation with moisture control, Chem. Pharm. Bull. 43 (1995) 1764–1771.
[12] S. Watano, T. Morikawa, K. Miyanami, Mathematical model in the kinetics of agitation fluidized bed granulation. Effects of moisture content, damping speed and operation time on granule growth rate, Chem. Pharm. Bull. 44 (1996) 409–415.
[13] N. Ouchiyama, T. Tanaka, Kinetic analysis and simulation of batch granulation, Ind. Eng. Chem. Process Des. Dev. 21 (1982) 29–35.
[14] S. Timoshenko, J.N. Goodier, Theory of Elasticity, 2nd Edition, McGraw-Hill, New York, 1951, pp. 372–377.
[15] B.J. Ennis, G. Tardos, R. Pfeffer, A microlevel-based characterization of granulation phenomena, Powder Technol. 65 (1991) 257–272.
[16] A.A. Adetayo, B.J. Ennis, A new approach to modelling granulation processes for simulation and control purposes, Powder Technol. 108 (2000) 202–209.
[17] H.G. Kristensen, P. Holm, T. Schaefer, Mechanical properties of moist agglomerates in relation to granulation mechanisms part II. Effects of particle size distribution, Powder Technol. 44 (1985) 239–247.
[18] R.L. Drake, T.J. Wright, The scalar transport equation of coalescence

theory: new families of exact solutions, J. Atmos. Sci. 29 (1972) 548–556.
[19] B. Pulvermacher, E. Ruckenstein, Similarity solutions of population balances, J. Colloid Interface Sci. 46 (1974) 428–436.
[20] A.A. Adetayo, J.D. Litster, S.E. Pratsinis, B.J. Ennis, Population balance modelling of drum granulation of materials with wide size distribution, Powder Technol. 82 (1995) 37–49.
[21] M.J. Hounslow, R.L. Ryall, V.R. Marshall, A discretized population balance for nucleation, growth, and aggregation, AIChE J. 34 (1988) 1821–1832.
[22] J.D. Litster, D.J. Smit, M.J. Hounslow, Adjustable discretized population balance for growth and aggregation, AIChE J. 41 (1995) 591–603.
[23] F. Gelbard, Y. Tambour, J.H. Seinfeld, Sectional representations for simulating aerosol dynamics, J. Colloid Interface Sci. 76 (1980) 541–556.
[24] T. Abberger, H. Egermann, Granule growth rates versus free humidity in fluid bed granulations, Eur. J. Pharm. Sci. 2 (1994) 110.
[25] T. Abberger, Zur Kinetik der Wirbelschichtgranulierung, Pharmazie 54 (1999) 611–613.
[26] Z. Ormos, K. Pataki, B. Csukas, Studies on granulation in a fluidized bed III. Calculation of the feed rate of granulating liquid, Hung. J. Ind. Chem. 1 (1973) 463–474.
[27] T. Abberger, J.A. Raneburger, H. Egermann, Instrumentation of a laboratory scale fluid-bed granulator for control of critical spray rate and of free moisture, Sci. Pharm. 64 (1996) 255–262.
[28] T. Abberger, H. Egermann, Die freie Feuchte als Kriterium für den Kornbildungsmechanismus bei der Wirbelschichtgranulierung, 11th Scientific Congress of the Austrian Pharmaceutical Society, Graz, Austria, 1994.
[29] A. Wade, P.J. Weller (Eds.), Handbook of Pharmaceutical Excipients 2nd Edition, Pharmaceutical Press, London, 1994, p. 485.
[30] B.B. Spencer, B.E. Lewis, HP-67/97 and TI-59 programs to fit the normal and log-normal distribution functions by linear regression, Powder Technol. 27 (1980) 219–226.
[31] H. Stricker (Ed.), Physikalische Pharmazie 3rd Edition, Wissenschaftliche Verlagsgesellschaft, Stuttgart, 1987, p. 478.
[32] R. Nimylowytsch, Diplomarbeit, University of Innsbruck, Innsbruck, 1995.
[33] N. Ouchiyama, T. Tanaka, Kinetic analysis and simulation of batch granulation, Ind. Eng. Chem. Process Des. Dev. 21 (1982) 29–35.
[34] L.X. Liu, J.D. Litster, S.M. Iveson, B.J. Ennis, Coalescence of deformable granules in wet granulation processes, AIChE J. 46 (2000) 529–539.
[35] H.G. Kristensen, Particle agglomeration in high shear mixers, Powder Technol. 88 (1996) 197–202.
[36] H.G. Kristensen, P. Holm, A. Jaegerskou, T. Schaefer, Granulation in high speed mixers part 4. Effect of liquid saturation on the agglomeration, Pharm. Ind. 46 (1984) 763–767.
[37] P. Holm, T. Schaefer, H.G. Kristensen, Granulation in high speed mixers part V. Power consumption and temperature changes during granulation, Powder Technol. 43 (1985) 213–223.
[38] C.-C. Huang, H.O. Kono, The granulation of partially prewetted alumina powders – a new concept in coalescence mechanism, Powder Technol. 55 (1988) 19–34.
[39] H.G. Kristensen, T. Schaefer, Granulations, in: J. Swarbrick, J.C. Boylan (Eds.), Encyclopaedia of Pharmaceutical Technology, 7, Marcel Dekker, New York, 1993, pp. 121–160.
[40] S.H. Schaafsma, P. Vonk, P. Segers, N.W.F. Kossen, Description of agglomerate growth, Powder Technol. 97 (1998) 183–190.
[41] B. Waldie, Growth-mechanism and the dependence of granule size on drop size in fluidized-bed granulation, Chem. Eng. Sci. 46 (1991) 2781–2785.
[42] T. Schaefer, O. Woerts, Control of fluidized bed granulation II. Estimation of droplet size of atomized binder solutions, Arch. Pharm. Chem. Sci. Ed. 5 (1977) 178–193.